Accepted Manuscript

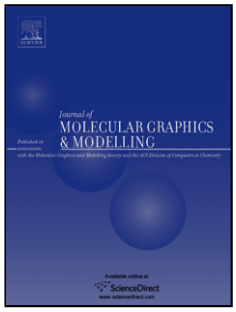

Title: Effect of the Solvent on the Conformational Behavior of the Alanine Dipeptide deduced from MD simulations

Authors: Jaime Rubio-Martinez, M. Santos Tomas, Juan J. Perez

PII: S1093-3263(17)30610-1
DOI: https://doi.org/10.1016/j.jmgm.2017.10.005
Reference: JMG 7044

To appear in: *Journal of Molecular Graphics and Modelling*

Received date: 8-8-2017
Revised date: 7-10-2017
Accepted date: 9-10-2017

Please cite this article as: Jaime Rubio-Martinez, M.Santos Tomas, Juan J.Perez, Effect of the Solvent on the Conformational Behavior of the Alanine Dipeptide deduced from MD simulations, Journal of Molecular Graphics and Modelling https://doi.org/10.1016/j.jmgm.2017.10.005

Effect of the Solvent on the Conformational Behavior of the Alanine Dipeptide deduced from MD simulations

Jaime Rubio-Martinez[1], M. Santos Tomas[2] and Juan J. Perez[3,*]

[1]Dept. of Physical Chemistry. Faculty of Chemistry, Universitat de Barcelona and the Institut de Recerca en Quimica Teorica i Computacional (IQTCUB). Mati i Franques 1-3. 08028 Barcelona, Spain

[2]Department of Architecture Technology. Universitat Politecnica de Catalunya. Av. Diagonal, 649, E-08028 Barcelona, Spain

[3]Department of Chemical Engineering. Universitat Politecnica de Catalunya- Barcelona Tech. Av. Diagonal, 647. 08028 Barcelona, Spain

*To correspondence must be addressed:

juan.jesus.perez@upc.edu

Graphical abstract

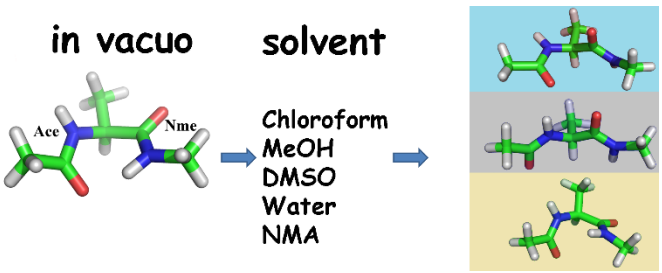

Highlights

- The manuscript describes a computational study of the differential conformational behavior of the alanine dipeptide in diverse solvents including chloroform, methanol, DMSO, water and methyl formamide.
- This study is important to understand the conformational behavior of peptides in diverse solvents, since the dialanine dipeptide is a model molecule to for peptides.
- The manuscript discusses the role of inter- and intra-molecular interactions to understand the differential behavior of the molecule in the diverse solvents.

- This work aims to shed light into the controversy found in the literature between experimental and theoretical calculations of the dialanine dipeptide in water.
- There has never been published a comparative computational study of the effect of the solvent on the molecule.

Abstract

In general, peptides do not exhibit a well-defined conformational profile in solution. However, despite the experimental blurred picture associated with their structure, compelling spectroscopic evidence shows that peptides exhibit local order. The conformational profile of a peptide is the result of a balance between intramolecular interactions between different atoms of the molecule and intermolecular interactions between atoms of the molecule and the solvent. Accordingly, the conformational profile of a peptide will change upon the properties of the solvent it is soaked. To get insight into the balance between intra- and intermolecular interactions on the conformational preferences of the peptide backbone we have studied the conformational profile of the alanine dipeptide in diverse solvents using molecular dynamics as sampling technique. Solvents studied include chloroform, methanol, dimethyl sulfoxide, water and N-methylacetamide. Different treatments of the solvent have been studied in the present work including explicit solvent molecules, a generalized Born model and using the bulk dielectric constant of the solvent. The diverse calculations identify four major conformations with different populations in the diverse solvents: the C_7^{eq} only sampled in chloroform; the C_5 or extended conformation; the polyproline (PII) conformation and the right-handed α-helix conformation (α_R). The results of present calculations permit to analyze how the balance between intra- and intermolecular interactions explains the populations of the diverse conformations observed.

Introduction

Peptide conformational features are intrinsically determined by its amino acid sequence and modulated by the environment. There are numerous examples reported in the literature where peptides adopt bound conformations different to those exhibited in solution [1,2] or peptides adopting different conformations in diverse solvents [3]. There are even examples where peptide segments adopt different conformations in diverse proteins, like the segment Asn-Ala-Ala-Ile-Arg-Ser that adopts a helical structure in phosphofructokinase and an extended conformation in thermolysin. In any case, the conformation peptides attain in diverse environments will correspond to the one with the lowest free energy. Alternatively, at the

molecular level the available conformational states of a peptide are the result of a balance between intramolecular interactions that dictate its intrinsic conformational features and intermolecular interactions with the environment [4]. A profound understanding of the interplay between intra- and intermolecular interactions is key to understand protein folding and at large, molecular recognition. To get insight into the balance between intra- and intermolecular interactions on the conformational preferences of the peptide backbone it is useful to use model molecules that can also be used to compare the performance of different methodologies. In this direction, the alanine dipeptide or (S)-2-acetylamino-N-methylpropanamide has been paradigmatically used for this purpose in the past [5] and it is the object of the present study.

The conformational profile of the alanine dipeptide both *in vacuo* as well as in aqueous solution has been thoroughly investigated in previous studies using diverse computational methods and experimental techniques [6-29]. Figure 1a shows a partition of the Ramachandran map used in the present work that permits to label the diverse conformations as a function of the dihedral angles ϕ and ψ and Figures 1b-1e show pictorially the geometries of the most populated conformations. Diverse computational studies identify the C_7^{eq} conformation as the lowest energy structure *in vacuo* followed by the extended C_5 and the C_7^{axial} conformations in increasing order of energy [7] in good agreement with available experimental results. Specifically, in a recent microwave spectroscopy study it was found that the alanine dipeptide populates both the C_7^{eq} and the C_5 conformations in a proportion 2:1 in the gas phase [18]. Interestingly, studies of the alanine dipeptide *in vacuo* are conclusive in discarding the right-handed α-helix (α_R) or the polyproline II (PII) conformations as low energy minima. This is an intriguing result since the former is often found in helical parts of globular proteins [19] and the latter is known to be the most abundant structure found in solution [20]. This result suggests that the environment created by either the rest of the protein or the solvent substantially modifies the conformational profile of the molecule.

Diverse experimental studies aimed to understand the conformational profile of the alanine dipeptide in water including IR and Raman spectroscopy [21, 22], as well as CD or NMR spectroscopy [23, 24] suggest that the molecule preferably adopts the PII conformation, being the C_5 and α_R conformations -in decreasing order of population- also attainable. Alternatively, diverse computational studies devoted to characterize the conformational profile of the alanine dipeptide in water identify conformations PII, C_5 and α_R as low energy minima. Unfortunately, different methods and approximations used to perform the calculations including basis set and level of theory at the *ab initio* level or force field parameters and water models at the molecular mechanics level provide a different energy rank order [13]. Despite this controversy, computational studies provide invaluable information about solvent distribution around the alanine dipeptide, pointing to the degree of hydration as the reason for the differential stability of the diverse conformations in water [25].

In order to get a deeper insight into the effect of the solvent on the conformational profile of the alanine dipeptide it seems interesting to extend these studies to different solvents. In a pioneering report combining NMR and CD spectroscopies, together with molecular mechanics calculations it was found that the C_7^{eq}

conformation was the dominant structure in non-polar solvents, whereas the α_R and PPII conformations were preferred conformations in polar ones [26]. More recently, IR and Raman spectroscopy studies showed compelling evidence that the most populated conformation of the alanine dipeptide in DMSO is the C_5 conformation followed by the PII, whereas the α_R conformation exhibits a similar population as in water [22]. From the theoretical side only a few calculations of the alanine dipeptide have been carried out in non-aqueous solvents. Thus, in a recent report, *ab initio* calculations at the Hartree-Fock and DFT levels using extended basis sets and with the solvent effect evaluated using an implementation of the COSMO reaction field method, identified the C_5 as the most stable conformation in chloroform, followed by the C_7^{eq}, PII and α_R in increasing order of energy [27]. Similarly, in a recent study combining NMR spectroscopy and DFT calculations, devoted to understand the conformational preferences of the alanine dipeptide in solvents of diverse polarity, it was concluded that populations of the C_5 and C_7^{eq} conformations decrease with the increasing polarity of the solvent, whereas the α_R conformation population shows the opposite trend [28]. More recently, in a QM/MM study devoted to understand the conformational behavior of the alanine dipeptide in ethanol-water mixtures it is shown that in contrast to the results in water, the α_R conformation exhibits lower energy than the PII conformation in ethanol [29].

Aimed at providing new insights into the features of the conformational profile of the alanine dipeptide in non-aqueous solvents we report in the present work the results of diverse molecular dynamics simulations using explicit solvent of the alanine dipeptide in diverse solvents including chloroform, methanol, dimethyl sulfoxide (DMSO), water and N-methylacetamide (NMA) and compare with the results obtained using a generalized Born model and the corresponding bulk dielectric constant of the solvent.

Methods

All the calculations reported in the present work were carried out by means of the AMBER14 software package [30] using the Sander and PMEMD programs in its CPU and GPU versions and the ff14SB force field [31]. The initial 3D structure of the alanine dipeptide was generated in its extended form using the Leap module of Ambertools16 [32].

The potential of mean force of the alanine dipeptide at 300K in diverse solvents including chloroform [33], methanol [33], DMSO [34], water (TIP3P) [35] and NMA [33] was computed using molecular dynamics simulations. Three approaches were used to simulate solvent effects: first, an explicit representation of solvent molecules; second, a representation of solvent effects by means of a generalized Born (GB); and third, an effective dielectric constant.

In the molecular dynamics simulations with explicit solvent the alanine dipeptide was placed in the center of a cubic box of solvent molecules with dimensions large enough that the minimum distance between any atom of the solute and the edge of the box was larger than 15 Å. Solvent molecules closer than 1.8 Å to any of the atoms of the alanine dipeptide were removed. Next, the systems were optimized by means of

10000 steps of the Steepest Descent algorithm to adapt the solvent-solute interface. The minimized structures were heated at 300 K at a constant rate of 30 K/10 ps. Then, 500 ps were performed at constant pressure to increase system density. Finally, four 3μs molecular dynamics simulations using different sets of initial velocities aimed at providing a better sampling for the same computational effort [36] were performed under the canonical ensemble using a Langevin thermostat with a collision frequency of 2 ps^{-1} for temperature control. Long-range electrostatic energy was computed using the Particle Mesh Ewald summation method [37] with a cutoff of 10 Å for non-bonded interactions. The SHAKE algorithm [38] was used to constrain bonds involving hydrogen atoms to allow the use of a 2 fs integration step.

For those calculations using a GB model and a bulk dielectric constant after the minimization step, four production molecular dynamics simulations 10μs longong, each of them using a different set of initial velocities, were performed under the same conditions. In this case the cutoff for the non-bonded interactions was increased to 12 Å to assure the inclusion of the maximum interatomic distance when the alanine dipeptide is in its extended conformation. GB calculations were carried out by means of the neck GB model that adds a geometrically based molecular volume correction term accounting for interstitial high dielectrics to pairwise GB models [39].

Analysis of the results was carried out using one snapshot every other picosecond that yields 500 snapshots/ns, i.e. 6 10^6 snapshots for the solvated MD trajectories (a total of 12 μs length) and 2010^6 snapshots for the non-solvated MD trajectories (a total of 40 μs length). Radial pair distribution functions were obtained using the cpptraj software [40] with a ΔR=0.1 Å .

Results and Discussion

As mentioned in the Methods section, for each of the solvents selected for the present study diverse MD simulations were carried out: first, in explicit solvent; second, using a GB method and third, using the bulk dielectric constant of the solvent. Below we describe the results obtained with the different approaches to discuss later the accuracy of the description of the conformational profile of the alanine dipeptide in the diverse solvents studied in the present work.

Low energy conformations

Figures 2a-2e show the Ramachandran maps corresponding to the MD simulations carried out in explicit solvent and the values of the (ϕ, ψ) angles for each of the low energy minima are listed in Table 1. Analysis of the Table indicates that chloroform is the only solvent where the C_7^{eq} conformation appears as a low energy minimum in the Ramachandran map, being also the most populated (Figure 2a). For the rest of the solvents with larger dielectric constants, despite the conformation is sampled, it does not appear as a low energy minimum, showing a rapid decrease of its population with the increasing dielectric constant (Figures 2b-2e). The comparative analysis also indicates that the population of the C_5 conformation decreases along

with the increase of the dielectric constant, although less dramatically than in the case of the C_7^{eq} conformation. Actually, the C_5 conformation exhibits a population ~35% in chloroform and decreases to ~10% for the rest of the solvents. Interestingly, new conformations emerge in the map along with the decreasing dielectric constant including the PII, α_R and α'. The PII and α_R are the most populated conformations for all the solvents other than chloroform with populations ~60%, and ~25%, respectively. Interestingly, in NMA the α_R population is higher than in the rest of the solvents (~35%) with a concomitant small decrease in the PII population (~50%), whereas the C_5 population remaining at ~10%.

The Ramachandran maps computed using a GB model are shown pictorially in Figures 3a-3e and the values of the (ϕ, ψ) angles for each of the low energy minima are listed in Table 2. In contrast to the results described above, the PII conformation is the most populated in all the solvents using this methodology. Its population in chloroform is ~43%, whereas in the rest of the solvents is a bit higher (~50%). The second most populated conformation in chloroform is the C_5 followed by the α_R with populations of ~34% and ~22%, respectively. In the rest of the solvents these two conformations are interchanged in such a way that the population of the C_5 conformation decreases to ~20% whereas that of the α_R increases to ~27%. Analysis of Figures 3a-3e together with the results of Table 2 indicate that the population of the C_7^{eq} conformation also decreases along with the increase of the dielectric constant, although it does not appear as a low energy minimum in any of the calculations not even in chloroform.

Simulations carried out using the bulk dielectric constant were conducted to understand the importance of screening the electrostatic interactions on the conformational profile of the alanine dipeptide. Figures 4a-4f show the Ramachandran maps of the alanine dipeptide computed at: a) ε=1.0 (*in vacuo*); b) ε=4.8 (chloroform); c) ε=32.6 (methanol); d) ε=46.7 (DMSO); e) ε=78.5 (water) and f) ε=191.3 (NMA), respectively and Table 3 lists the values of the ϕ and ψ angles of the corresponding low energy minima for each of the different dielectric constants. Analysis of Figures 4a-4f together with the results of Table 3 suggests that the population of the C_7^{eq} conformation also decreases dramatically along with the increase of solvent dielectric constant. Actually, a small increase in the dielectric constant to 4.8 -that of chloroform- produces a dramatic decrease on the population of this conformation. Despite the conformation is sampled in chloroform (Figure 4b) and in methanol (Figure 4c), it cannot be identified as a low energy minimum. Also as found above, there is a smoother decrease in the population of the C_5 conformation. Specifically, the population decreases from ~50% in chloroform to ~35% for the rest of the solvents. Interestingly, the loss of C_7^{eq} population is associated with the emergency of new conformations including the PII, α_R and α', in increasing order of energy. Thus, apart from the *in vacuo* calculation for the rest of calculations the most populated conformations are the PII and the C_5, with the former being the most favorable in solvents with dielectric constant of methanol and higher exhibiting a population ~45%. Finally, other conformations have minimal populations. Specifically, the α_R conformation exhibits a population of ~10% in all the calculations and the α' ~5%.

A comparative analysis of Tables 1-3 suggests that the diverse methodologies used in the present study capture the decreasing population of the C_7^{eq} conformation along with solvent dielectric constant increase. This result is expected since the hydrogen bond between the carbonyl oxygen of the acetyl group and the hydrogen of the N-methylamide moiety at the C-terminus that characterizes this conformation (see Figure 1b) is expected to weaken with the increasing dielectric constant. Moreover, present calculations also coincide to point that this conformation is only relevant *in vauo* (Figure 4a) and in chloroform (Figure 2a). In chloroform the C_7^{eq} is the lowest energy minimum with a population of ~46% followed by the C_5 with a population of ~37% and the PII conformation with much lower population (~10%). None of the other two maps computed with a low dielectric constant either using the GB model (Figure 3a) or using the bulk dielectric constant (Figure 4b) exhibits the C_7^{eq} as low energy minimum. Specifically, in the calculation using a GB model the lowest energy conformation is the PII, whereas in the bulk dielectric calculations the C_5 appears as the lowest energy minimum.

Similarly, the calculations reported in the present work indicate a decreasing population of the C_5 conformation along with solvent dielectric constant increase, although with a slower rate than in the case of the C_7^{eq} conformation. Specifically, in explicit solvent calculations the population drops from a ~38% population in chloroform to ~10% for the rest of the solvents; using a GB model it decreases from ~34% to ~20% for the rest of the solvents and using the bulk dielectric from ~50% to ~35% for the rest of the solvents. This observed decrease can be explained as the result of weakening the electrostatic interactions between the two consecutive peptide bond dipole moments that can be considered an important component of C_5 conformation stability. However, the population of the C_5 conformation is much higher in the bulk dielectric calculations than in implicit or explicit calculations, suggesting that the screening effect on the electrostatic interactions is not the only factor that destabilizes this conformation.

Finally, in regard to the α_R conformation, analysis of Figures 2a-2e and Table 1 suggests an increasing population along with solvent dielectric constant in the explicit solvent calculations. Specifically, the conformation is not sampled in chloroform, but exhibits ~25% population in methanol, DMSO and water, increasing to ~37% in NMA. Similarly, in implicit solvent calculations (Figures 3a-3e and Table 2) the population increases smoothly along with the dielectric constant: from a ~22% in chloroform to ~27% in the rest of the solvents. In contrast, in the calculations carried out with bulk dielectric constant (Figures 4b-4f and Table 3) the population of this conformation remains a ~10% in all the solvents. These results suggest that the stabilization of the α_R conformation must be due to explicit interactions with the solvent.

Solvent distribution

Analysis of the solvent distribution around the dipeptide alanine computed from the simulations carried out in explicit solvent provides further insight into the solute-solvent interactions. First is necessary to consider that the five solvents used in the present calculations are of diverse nature. Specifically, methanol, water and NMA exhibit proton accepting and donor centers. Similarly, chloroform exhibits a proton donor center located

in the hydrogen and hydrogen bond accepting centers located on the chlorine atoms. In contrast to the rest of the solvents, DMSO exhibits only a proton accepting center. Solvents can interact with the polar groups of the alanine dipeptide. Specifically, the proton accepting centers located at the acetyl and the alanine carbonyl oxygens and the proton donor centers located at the amide hydrogens of alanine and the N-methylamide.

Figures 5a-5d show the radial pair distribution function for the interaction between the alanine carbonyl oxygen and a proton donor center of the solvent molecule for the PII, α_R and C_5 conformations. In the case of methanol (Figure 5b) and NMA (Figure 5d) the radial pair distributions show the same profile: a first solvation shell at ~1.9 Å with differential solvent density that follows the order PII> α_R>C_5. This effect can be observed more dramatically in NMA calculations. Interestingly, the radial pair distribution in water shows a first solvation shell with the same characteristics found in methanol and NMA but also exhibits a second peak at ~3.2 Å. Finally, in the case of chloroform (Figure 5a) the radial pair distribution shows a peak at a longer distance ~2.3 Å for the conformations C_7^{eq}, C_5, P_{II} andC_7^{ax}, with differential solvent density that follows the order C_7^{eq} ~ C_7^{eq} ~ P_{II} >C_5,.

Similarly, Figures 6a-6d show the radial pair distribution function for the interaction between the acetyl carbonyl oxygen and a proton donor center of the solvent molecule for the PII, α_R and C_5 conformations. The radial pair distributions for methanol (Figure 6b), water (Figure 6c) and NMA (Figure 6d) are similar and resemble to those of the alanine carbonyl oxygen discussed above (Figures 5b-5d), although in this case peak heights are similar for the three solvents. In contrast, the radial pair distribution function for chloroform (Figure 6a) shows remarkable differences in regard that of the alanine carbonyl oxygen discussed above (Figure 5a). In this case, the acetyl carbonyl oxygen appears with higher solvent density in the C_5 conformation than in the C_7^{eq}. This differential behavior can be easily explained as due to the role of the acetyl carbonyl oxygen involved in a hydrogen bond to stabilize the C_7^{eq} conformation.

Figures 7a-7e show the radial pair distribution function for the interaction between the alanine amide hydrogen and a proton accepting center of the solvent molecule for the PII, α_R and C_5 conformations. The distributions for the diverse solvents show two peaks. In the case of methanol (Figure 7b), DMSO (Figure 7c), water (Figure 7d) and NMA (Figure 7e) the first peak is at ~2 Å, whereas the second is at ~5.6 Å. For all the conformations the first peak of the C_5 conformation is the shortest, whereas the difference between the P_{II} and the α_R conformations is not significant. Interestingly, the radial pair distributions for the α_R conformation in DMSO and NMA do not exhibit a second peak. The radial pair distribution of water presents the interesting feature of having the second peak higher than the first. This feature can also be observed in the distribution computed with chloroform (Figure 7a) where the first peak appears at ~3 Å and the second ~6.3 Å.

Finally, Figures 8a-8e show the radial pair distribution function for the interaction between the N-methylamide hydrogen and a proton accepting center of the solvent molecule for the PII, α_R and C_5 conformations. The plots (Figures 8b-8e) present two peaks: one at ~2 Å and the second is much wider than in the radial pair distributions discussed above, located between 5 and 6 Å. Interestingly, in this case the PII

and the C_5 conformations show the same peak height, whereas the α_R conformation is lower. In the case of chloroform (Figure 8a) the distribution for the diverse conformations shows a differential behavior. Thus, in the case of the PII conformation the distribution shows a first peak at around 2.8 Å. In the case of the C_5 conformation the distribution shows a shoulder rather than a peak also ~2.8 Å, whereas the rest of the conformations present also a shoulder about one angstrom farther. Moreover, all the conformations exhibit a second peak between 6-7 Å.

Taken these results together suggest that the increase of solvent dielectric constant destabilizes the C_7^{eq} and C_5 conformations due to the weakening of the electrostatic interactions. The C_7^{eq} conformation is stabilized by an intramolecular hydrogen bond between the carbonyl oxygen of the acetyl group and the amide hydrogen of the N-methylamine moiety that gives origin to the C_7 cycle. At the dielectric constant of chloroform (4.8) this interaction is much weakened in such a way that the hydrogen bond is hardly stable as shown in the bulk dielectric calculation shown in Figure 3b. However, the fact that the conformation is found as the lowest energy minimum in the explicit solvent calculations suggests a stabilizing role of the solvent molecules. Actually, Figures 6a and 8a show that the alanine dipeptide atoms involved in the intramolecular hydrogen bond are surrounded by a lower number of solvent molecules than in other conformations, whereas for the alanine carbonyl oxygen (Figure 7a) and the hydrogen amide (Figure 9a) exhibit the same density of solvent molecules for all conformations. In other words, solvent molecules form intermolecular interactions with all four polar groups of the solute in such a way that they do not disrupt the intramolecular hydrogen bond. In regard to the C_5 conformation the decrease in population observed along with the increase of solvent dielectric constant is smoother than with the C_7^{eq}. This effect can also be explained to be due to a weakening of the electrostatic interactions that in this case are the weaker dipole-dipole interactions between the two peptide bond dipole moments. Inspection of Figures 4b-4f suggests that the effect is not as dramatic as in the case of the C_7^{eq} conformation. Moreover, the decreasing stability of this conformation cannot be compensated by intermolecular interactions with the solvent as deduced from the inspection of Figures 5-8 that show that in many cases solute polar groups are less surrounded of solvent molecules than in other conformations. This must be due to the geometry of this conformation that does not allow solvent molecules to reside within the space formed by the C_5 cycle. In contrast, the PII conformation can be considered as a distorted C_5 conformation where solvent molecules can adequately surround solute solvent groups. These results agree with previous *Ab initio* studies of the alanine dipeptide surrounded with a few water molecules [41]. This can explain that once the intramolecular electrostatic interactions are not as important due to the decreasing dielectric constant, the importance of forming intermolecular interactions with the solvent gets its importance and consequently, the PII conformation gains population. Finally, it needs to be considered that the alanine dipeptide is not long enough to form a typical α-helical hydrogen bond that stabilizes the structure. Accordingly, the stability of this conformation in the alanine dipeptide can be considered to be due to solvent effects exclusively since the increase of the dielectric constant does not alter the population of this

conformation as it can be seen in Table 3. Indeed, molecular simulations carried out on Gly-Ala-Gly in water show an increase population of the α_R conformation in comparison to alanine dipeptide calculations [42, 43].

Comparison with experimental results

There is not much experimental information available on the conformational profile of the alanine dipeptide in chloroform. Actually, in a pioneering study involving CD and NMR spectroscopies together with computational studies, it was concluded that in non-polar solvents the molecule adopts similar conformations as *in vacuo* [27]. Comparison of Figures 2a, 3a and 4b with Figure 4a clearly indicates that the experimental result is only reproduced in the explicit solvent calculations. Thus, in the map computed with a GB method despite the α_R basin appears distorted towards the C_7^{eq} conformation it does not appear as an energy minimum. In contrast, the PII and the C_5 appear as low energy minima with similar populations: ~43% and ~34%, respectively. Similar results are obtained in an *ab initio* study at the Hartree-Fock and DFT levels using extended basis sets and with solvent effects evaluated using an implementation of the COSMO reaction field. In that study the authors concluded that the C_5 is the most stable conformation in chloroform [28]. Finally, the calculations performed using the bulk dielectric of chloroform show that a small increase in the dielectric constant to 4.8 produces a dramatic decrease of the C_7^{eq} conformation population. This suggests that the stability of this conformation must be related to specific features related to the solvation process.

In regard to methanol the three methods point to the PII conformation as being the lowest energy conformation with populations ~50% or higher (Figures 2b, 3b and 4c). In this case, explicit solvent and the generalized Born model calculations agree identifying the α_R as the second most populated conformation (~26%), being the C_5 the third most populated, although with differential populations: in explicit solvent is ~10% and using the generalized Born method is ~21%. Moreover, the α' conformation is also identified in explicit solvent calculations with a small population of ~3%. In contrast, calculations carried out using the bulk dielectric (Figure 4c) show an energy rank order with the C_5 and the α_R inverted, with populations ~38% and ~10%, respectively. Unfortunately, there are not experimental studies available in this solvent.

In regard to DMSO, explicit solvent and the generalized Born method provides the same results (Figures 3c and 4c, respectively). Specifically, the PII conformation is the most populated (~50%), followed by the α_R with a population ~25%. The third most populated conformation in both calculations is the C_5, although there are differences in the population. In explicit solvent the population is ~13%, clearly smaller than α_R, whereas the generalized Born calculation gives ~21%, similar to that of the α_R conformation. Moreover, the explicit solvent calculation identifies the α' conformation as attainable with ~9% population. Alternatively, the Ramachandran map of the calculation performed using a relative dielectric constant of 46.7 is shown in Figure 4c. As described before it shows the PII conformation as the lowest energy minimum but in contrast to the previous calculations, the energy rank order of conformations C_5 and α_R is inverted with populations of ~38 and ~10%, respectively. Moreover, when the populations of the PII, α_R and C_5 conformations found in water and DMSO are compared (Tables 1), it can be inferred a discrete decrease in the population of the PII

conformation with an accompanying increase in the population of the C_5 conformation in DMSO compared to water. In contrast the population of the α_R conformation is similar. Inspection of Tables 1 and 3 suggests that the effect is due to the difference of dielectric constant. However, solvation may also play a role. In fact, it should be bared in mind that the DMSO molecule does not have any proton donor and consequently, can only form intermolecular hydrogen bonds with the amide hydrogens of the solute molecule. Accordingly, it does not pay off to distort the C_5 conformation into the PII to allow better contact with solvent molecules. This trend is captured in IR and Raman spectroscopy studies, although experimental results suggest a much more dramatic effect than reflected in the calculations [22].

In water, calculations using explicit solvent and the generalized Born model qualitatively show the same results (Figures 3d and 4d, respectively). Specifically, the PII appears as the most populated conformation followed by the α_R and C_5, though the expected populations differ in the two calculations. Thus, whereas in explicit solvent the populations are: ~60%; ~27%; ~10%, respectively, in the generalized Born model are ~53%; ~27%; ~20%, showing clear difference in the relative population of PII/C_5 conformations. These results agree well with the results of QM/MM calculations that include correlation at the MP2 level [17]. Alternatively, Figure 4e shows the Ramachandran map of the alanine dipeptide computed using a relative dielectric constant of 78.5. As can be seen the map shows the PII conformation as the lowest energy minimum with a population ~46%, but in contrast to previous calculations the C_5 has a higher population (~38%) than the α_R conformation (~10%). Interestingly, experimental findings coincide well with these results. Specifically, IR and Raman spectroscopy [22, 23], as well as CD and NMR spectroscopy [24, 25] suggest that the molecule preferably adopts a PII conformation followed by the C_5 and α_R conformations, in increasing order of energy.

In the case of NMA both explicit solvent calculations and calculations using the generalized Born model qualitatively show the same results (Figures 3e and 4e, respectively): the PII appears as the most populated conformation followed by the α_R and C_5. Despite the energy rank order of the conformation is the same the populations are different. Whereas the population of the PII conformation is about 50% in both calculations, in the explicit solvent calculations the α_R/C_5 ratio is nearly 4:1 and in the generalized Born calculations is approximately 1.5:1. Alternatively, Figure 2f shows the Ramachandran map of the alanine dipeptide computed using a relative dielectric constant of 191.3. As found in water, the PII conformation is identified as the lowest energy minimum followed by the C_5 and at higher energies the α_R with populations ~46%, ~38% and ~10% respectively. Comparison of these results with those computed in water indicates that the relative population of the α_R conformation is the same, whereas the population of the PII decreases and the C_5 increases.

Conclusions

In the present work we have carried out MD studies of the alanine dipeptide in solvents of different dielectric constant namely, chloroform, methanol, DMSO, water and NMA and analyze the populations of the

diverse conformations sampled. We have also carried out MD calculations of the dialanine dipeptide using a generalized Born method with each of the dielectric constants to understand the differences with explicit solvent calculations. Finally, we have also carried out MD calculations of the dialanine dipeptide using the bulk dielectric constant of the solvent to understand the effect of screening the electrostatic interactions on the populations of the molecule.

The most populated conformation in chloroform is the C_7^{eq} as also found in *in vacuo* calculations. In the rest of the solvents, the population of this conformation decreases along with the increasing dielectric constant as a consequence of the weakening of the hydrogen bond between the acetylcarbonyl oxygen and the N-methylamide hydrogen. Similarly, the population of the C_5 conformation that is the second most populated in chloroform, also decreases along with the increasing dielectric constant although much more smoothly than in the previous case. This effect may also be due to the weakening of the electrostatic interactions, although in DMSO the conformation exhibits higher population than expected due to solvation effects. Actually, present calculations in explicit solvent show a discrete increase, although it has been claimed that this increase should be more dramatic as deduced from the results of spectroscopic studies [22]. The other two important conformations sampled in the diverse solvents are the PII and the α_R. The former can be considered as a distortion of the C_5 conformation being the result of a balance between preserving the dipole-dipole intramolecular interaction between the two consecutive peptide bonds and increase the solvation effects by allowing solvent molecules to produce better intermolecular interactions with the solute molecule. This conformation is barely sampled in chloroform with a population of ~10%. In regard to the α_R conformation it needs to be considered that the alanine dipeptide is not long enough to form a typical α-helical hydrogen bond that stabilizes the structure. Accordingly, the stability of this conformation can be considered to be due to solvent effects exclusively.

References

1. C. Weber, G. Wider, B. Von Freyberg, R. Traber, W. Braun, H. Widmer and K.Wuthrich, NMR structure of cyclosporin A bound to cyclophilin in aqueous solution, Biochemistry, 30 (1991) 6563-6574.
2. J.J. Perez, M.S. Tomas and J. Rubio-Martinez, Assessment of the sampling performance of multiple-copy dynamics versus a unique trajectory, J. Chem. Infor. Model. 56 (2016) 1950-1962.
3. S. K. Awasthi, S.C. Shankaramma, S. Raghothama and P. Balaram, Solvent-induced beta-hairpin to helix conformational transition in a designed peptide, Biopolymers. 58 (2001) 465-476
4. C. Soriano-Correa, F. J. Olivares del Valle, A. Munoz-Losa, I. Fdez. Galvan, M. E. Martin and M. A. Aguilar, Theoretical study of the competition between intramolecular hydrogen bonds and solvation in the Cys-Asn-Ser tripeptide, J. Phys. Chem. B 114 (2010) 8961–8970.
5. F. Avbelj, S.G. Grdadolnik, J. Grdadolnik and R. L. Baldwin, Intrinsic backbone preferences are fully present in blocked amino acids, Proc. Natl. Acad. Sci. USA 103 (2006) 1272–1277.
6. T. Head-Gordon, M. Head-Gordon, M. J. Frisch, C. L. Brooks and J. A. Pople, Theoretical Study of Blocked Glycine and Alanine Peptide Analogues, J. Am. Chem. Soc. 113 (1991) 5989-5997.
7. I. R. Gould, W. D. Cornell and I. H. Hillier, A quantum Mechanical Investigation of the Conformational Energetics of the Alanine and Glycine Dipeptides in the Gas Phase and in Aqueous Solution, J. Am. Chem. Soc. 116 (1994) 9250-9256.
8. M. D. Beachy, D. Chasman, R. B. Murphy, T. A. Halgren and R. A. Friesner, Accurate ab initio quantum chemical determination of the relative energetics of peptide conformations and assessment of empirical force fields, J. Am. Chem. Soc. 119 (1997) 5908–5920.
9. R. Vargas, J. Garza, B. P. Hay and D. A. Dixon, Conformational Study of the Alanine Dipeptide at the MP2 and DFT Levels, J. Phys. Chem. A 106 (2002) 3213-3218.
10. A. Perczel, D. Farkas, I. Jakli, I. A. Topol and I. G. Csizmadia, Peptide Models. XXXIII. Extrapolation of Low-Level Hartree–Fock Data of Peptide Conformation to Large Basis Set SCF, MP2, DFT, and CCSD(T) Results. The Ramachandran Surface of Alanine Dipeptide Computed at Various Levels of Theory, J. Comput. Chem. 24 (2003) 1026–1042.
11. Z.-X. Wang and Y. Duan, Solvation Effects on Alanine Dipeptide: A MP2/cc-pVTZ//MP2/6-31G** Study of (ϕ, ψ) Energy Maps and Conformers in the Gas Phase, Ether, and Water, J. Comput. Chem. 25 (2004)1699–1716.
12. A.T. Tzanov, M. A. Cuendet and M. E. Tuckerman, How Accurately Do Current Force Fields Predict Experimental Peptide Conformations? An Adiabatic Free Energy Dynamics Study, J. Phys. Chem. B 118 (2014) 6539−6552.
13. R. B. Best, X. Zhu, J. Shim, P. E. Lopes, J. Mittal, M. Feig and A. D. MacKerell, Jr, Optimization of the Additive CHARMM All-Atom Protein Force Field Targeting Improved Sampling of the Backbone ϕ,ψ and Side-Chain χ1 and χ2 Dihedral Angles, J. Chem. Theory Comput. 8 (2012) 3257−3273.

14. N. Schmid, A. P. Eichenberger, A. Choutko, S. Riniker, M. Winger, A. E. Mark and W. F. van Gunsteren, Definition and Testing of the GROMOS Force-Field Versions 54A7 and 54B, Eur. Biophys. J. 40 (2011) 843−856.
15. G. A. Kaminski, R. A. Friesner, J. Tirado-Rives and W. L. Jorgensen, Evaluation and Reparametrization of the OPLS-AA Force Field for Proteins via Comparison With Accurate Quantum Chemical Calculations on Peptides, J. Phys. Chem. B 105 (2001) 6474−6487.
16. F. F. García-Prieto, I. F. Galván, M. A. Aguilar and M. E. Martín, Study on the conformational equilibrium of the alanine dipeptide in water solution by using the averaged solvent electrostatic potential from molecular dynamics methodology, J. Chem. Phys. 135 (2011) 194502.
17. J. Rubio-Martinez and J. J. Perez, Effect of the solvent on the conformational Behavior of the alanine dipeptide in Explicit Solvent Simulations, In "Theoretical & Quantum Chemistry at the Dawn's End of 21st Century". R. Carbó-Dorca and T. Chakraborty (Eds.). Apple Academic Press, Waretown, NJ (USA), in press.
18. C. Cabezas, M. Varela, V. Cortijo, A.I. Jimenez, I. Pena, A. M. Daly, J. C. Lopez, C. Cativiela and J. L. Alonso, The alanine model dipeptide Ac-Ala-NH2 exists as a mixture of Ceq7 and C5 conformers, Phys. Chem. Chem. Phys. 15 (2013) 2580-2585.
19. S. Novmöller, T. Zhou and T.Ohlson, Conformations of amino acids in proteins, Acta Crystallogr., Sect. D 58 (2002) 768-776.
20. A. Hagarman, T. J. Measey, D. Mathieu, H. Schwalbe and R. Schweitzer-Stenner, Intrinsic Propensities of Amino Acid Residues in GxG Peptides Inferred from Amide I Band Profiles and NMR Scalar Coupling Constants, J. Am. Chem. Soc. 132 (2010) 540−551.
21. Y. S. Kim, J. Wang, and R. M. Hochstrasser. Two-Dimensional Infrared Spectroscopy of the Alanine Dipeptide in Aqueous Solution, J. Phys. Chem. B 109 (2005) 7511-7521.
22. J. Grdadolnik, V. Mohacek-Grosev, R. L. Baldwin and F. Avbelj, Populations of the three major backbone conformations in 19 amino acid dipeptides, Proc. Natl. Acad. Sci. USA, 108 (2011) 1794–1798.
23. S. E. Toal, D. Meral, D. Verbano, B. Ubanc and R. J. Schweitzer-Stenner, pH-Independence of Trialanine and the Effects of Termini Blocking in Short Peptides: A Combined Vibrational, NMR, UVCD, and Molecular Dynamics Study, J. Phys. Chem. B 117 (2013) 3689−3706.
24. A. Mirtic, F. Merzel and J. Grdadolnik, The Amide III Vibrational Circular Dichroism Band as a Probe to Detect Conformational Preferences of Alanine Dipeptide in Water, Biopolymers 101 (2014) 814–818.
25. D. Meral, S. Toal, R. Schweitzer-Stenner and B. Urbanc, Water-Centered Interpretation of Intrinsic pPII Propensities of Amino Acid Residues: In Vitro-Driven Molecular Dynamics Study, J. Phys. Chem. B 119 (2015) 13237−13251.
26. V. Madison and K. D. Kopple, Solvent-Dependent Conformational Distributions of Some Dipeptides, J. Am. Chem. Soc. 102 (1980) 4855-4863.

27. Y. K. Kang, Conformational Preferences of Non-Prolyl and Prolyl Residues, J. Phys. Chem. B 110 (2006) 21338-21348.
28. R. A. Cormanich, M. Bühlb and R. Rittner, Understanding the conformational behaviour of Ac-Ala-NHMe in different media. A joint NMR and DFT study, Org. Biomol. Chem. 13 (2015) 9206-9213.
29. G. G. Almeida, J. M. M. Cordeiro, M. E. Martín and M. A. Aguilar, Conformational Changes of the Alanine Dipeptide in Water−Ethanol Binary Mixtures, J. Chem. Theory Comput. 12 (2016) 1514−1524.
30. D. Case, V. Babin, J. Berryman, R. Betz, Q. Cai, D. Cerutti, T.E. Cheatham, III., T. Darden, R. Duke, H. Gohlke, A. Goetz, S. Gusarov, N. Homeyer, P. Janowski, J. Kaus, I. Kolossvary, A. Kovalenko, T. Lee, S. LeGrand, T. Luchko, R. Luo, B. Madej, K. Merz, F. Paesani, D. Roe, A. Roitberg, C. Sagui, R. Salomon-Ferrer, G. Seabra, C. Simmerling, W. Smith, J. Swails, R. Walker, J. Wang, R. Wolf, X. Wu and P. Kollman, AMBER14, 2014, University of California, San Francisco.
31. J.A. Maier, C. Martinez, K. Kasavajhala, L. Wickstrom, J.E. Hauser and C. Simmerling, f14SB: Improving the Accuracy of Protein Side Chain and Backbone Parameters from ff99SB, J. Chem. Theory Comput. 11 (2015) 3696-3713.
32. D.A. Case, R.M. Betz, D.S. Cerutti, T.E. Cheatham, III, T.A. Darden, R.E. Duke, T.J. Giese, H. Gohlke, A.W. Goetz, N. Homeyer, S. Izadi, P. Janowski, J. Kaus, A. Kovalenko, T.S. Lee, S. LeGrand, P. Li, C., Lin, T. Luchko, R. Luo, B. Madej, D. Mermelstein, K.M. Merz, G. Monard, H. Nguyen, H.T. Nguyen, I., Omelyan, A. Onufriev, D.R. Roe, A. Roitberg, C. Sagui, C.L., Simmerling, W.M., Botello-Smith, J. Swails, R.C. Walker, J. Wang, R.M. Wolf, X. Wu, L. Xiao and P.A. Kollman, AMBER16, 2016. University of California, San Francisco.
33. P. Cieplak, J. Caldwell and P. Kollman, Molecular mechanical models for organic and biological systems going beyond the atom centered two body additive approximation: Aqueous solution free energies of methanol and N-methyl acetamide, nucleic acid base, and amide hydrogen bonding and chloroform/water partition coefficients of the nucleic acid bases, J. Comput. Chem. 22 (2001) 1048–1057.
34. H. Liu, F. Müller–Plethe and W. F. van Gunsteren, Force Field for Liquid Dimethyl Sulfoxide and Physical Properties of Liquid Dimethyl Sulfoxide Calculated Using Molecular Dynamics Simulation, J. Am. Chem. Soc. 117 (1995) 4363-4366.
35. W. Jorgensen, J. Chandrasekhar, J. Madura and M. Klein, Comparison of simple potential functions for simulating liquid water, J. Chem. Phys. 79 (1983) 926–935.
36. J.J. Perez, M.S. Tomas and J. Rubio-Martinez, Assessment of the Sampling Performance of Multiple-Copy Dynamics versus a Unique Trajectory, J. Chem. Inf. Model. 56 (2016) 1950-1962
37. T. Darden, D. York and L. Pedersen, Particle Mesh Ewald: An N.Log(N) Method for Ewald Sums in Large Systems, J. Chem. Phys. 98 (1993)10089-10092.
38. J-P. Ryckaert, G. Ciccotti and H.J.C. Berendsen, Numerical Integration of the Cartesian Equations of Motion of a System with Constraints: Molecular Dynamics of n-alkanes, J. Comput. Phys. 23 (1977) 327–341

39. J. Mongan, C. Simmerling, J. A. McCammon, D. Case and A.Onufriev, A. Generalized Born with a simple, robust molecular volume correction, J. Chem. Theory Comput. 3 (2007) 156–169.
40. D. R. Roe and T. Cheatham, III, PTRAJ and CPPTRAJ: Software for Processing and Analysis of Molecular Dynamics Trajectory Data, J. Chem. Theory Comput. 9 (2013) 3084–3095.
41. G. Lanza and M. A. Chiacchio. Ab Initio MP2 and Density Functional Theory Computational Study of AcAlaNH2 Peptide Hydration: A Bottom-Up Approach, Chem. Phys. Chem. 15 (2014) 2785 – 2793.
42. D. Meral, S. Toal, R. Schweitzer-Stenner and B. Urbanc. Water-Centered Interpretation of Intrinsic pPII Propensities of Amino Acid Residues: In Vitro-Driven Molecular Dynamics Study, J. Phys. Chem. B 119 (2015) 13237−13251.
43. N. V. Ilawe, A. E. Raeber, R. Schweitzer-Stenner, S. E. Toal and B. M. Wong, Assessing backbone solvation effects in the conformational propensities of amino acid residues in unfolded peptides. Phys. Chem. Chem. Phys. 17 (2015) 24917—24924.

Captions to the Figures

Figure 1.- a)Partition of the Ramanchandran map in 120ºx120º regions corresponding to the different catchment regions of the alanine dipeptide potential of mean force including the labeling of the different conformations used in the present work. b-e) pictorial representation of the most populated conformations: b)C_7^{eq}; c)C_5; d)PII and e) α_R.

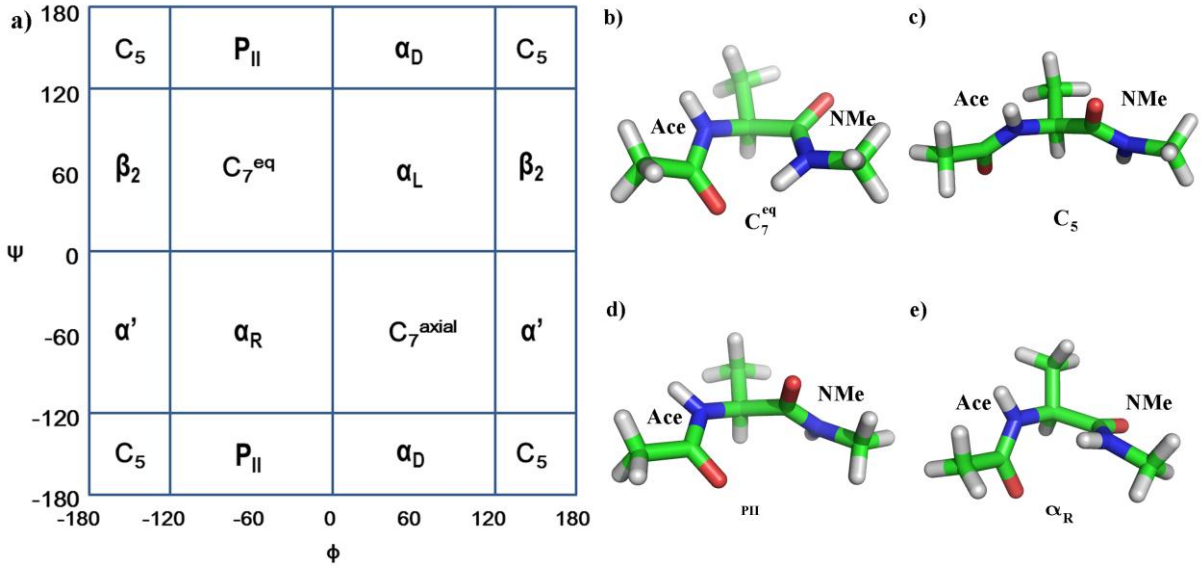

Figure 2.- Potential of mean force (in kcal/mole) of the alanine dipeptide in explicit solvent calculations. a) chloroform; b) methanol; c) DMSO; d) water; e) NMA.

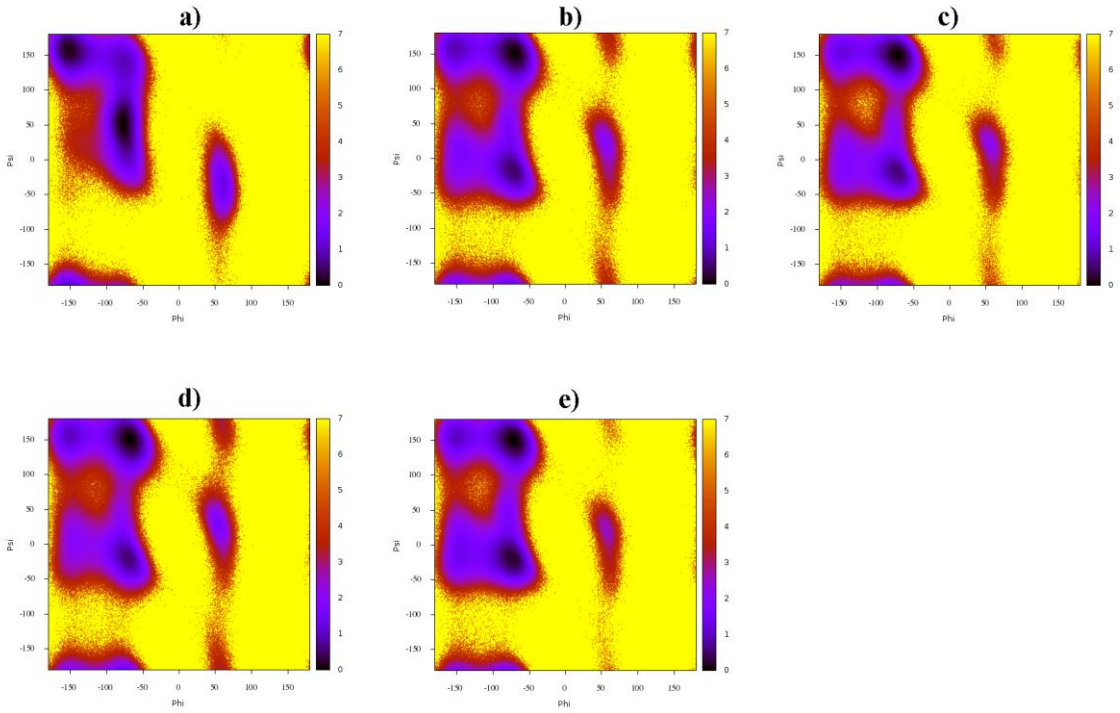

Figure 3.- Potential of mean force (in kcal/mole) of the alanine dipeptide using a Generalized Born method. a) chloroform; b) methanol; c) DMSO; d) water; e) NMA.

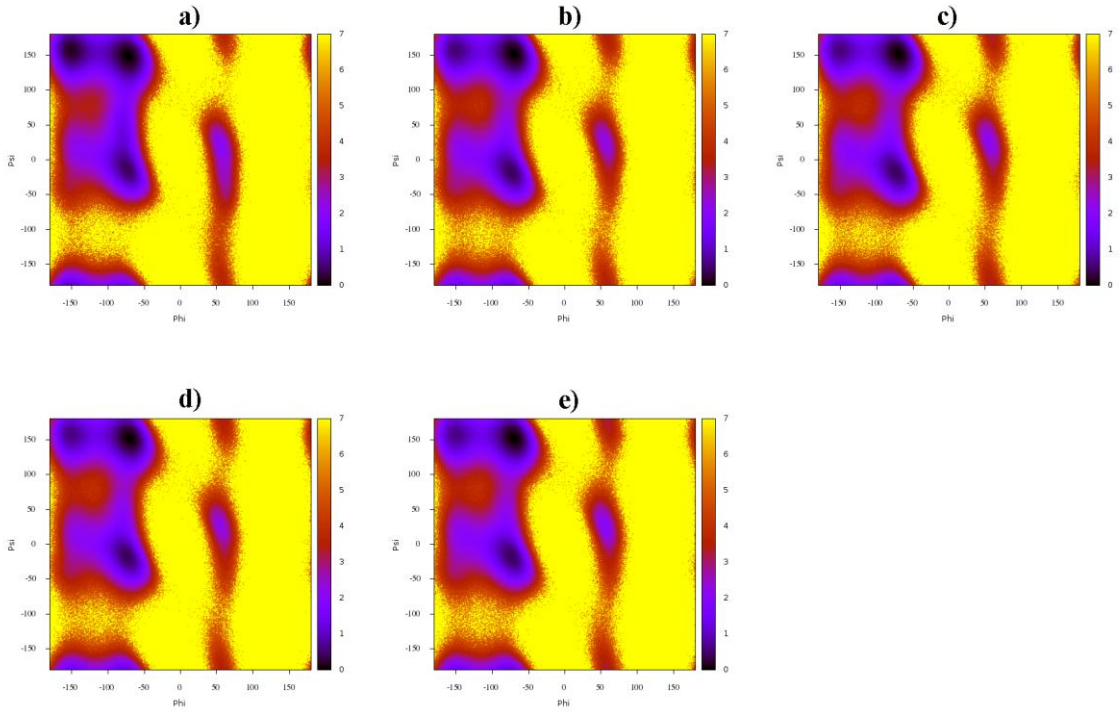

Figure 4.- Potential of mean force (in kcal/mole) of the alanine dipeptide using a bulk dielectric constant. a) ε=1 (vacuum); b) ε=4.8 (chloroform); c) ε=32.6 (methanol); d) ε=46.7 (DMSO); e) ε=78.5 (water) and f) ε=191.3 (NMA).

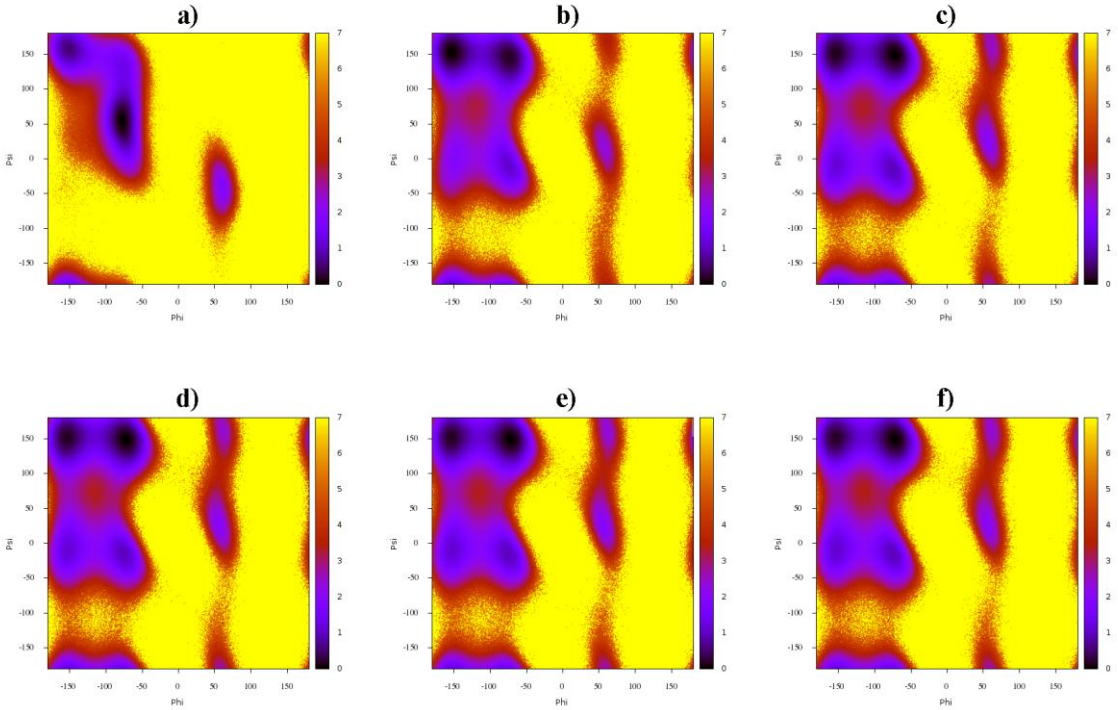

Figure 5.- Radial pair distribution function for the interaction between the alanine carbonyl oxygen and a proton donor center of the solvent molecule for the PII, αR and C5 conformations. a) chloroform; b) methanol; c) water; d) NMA

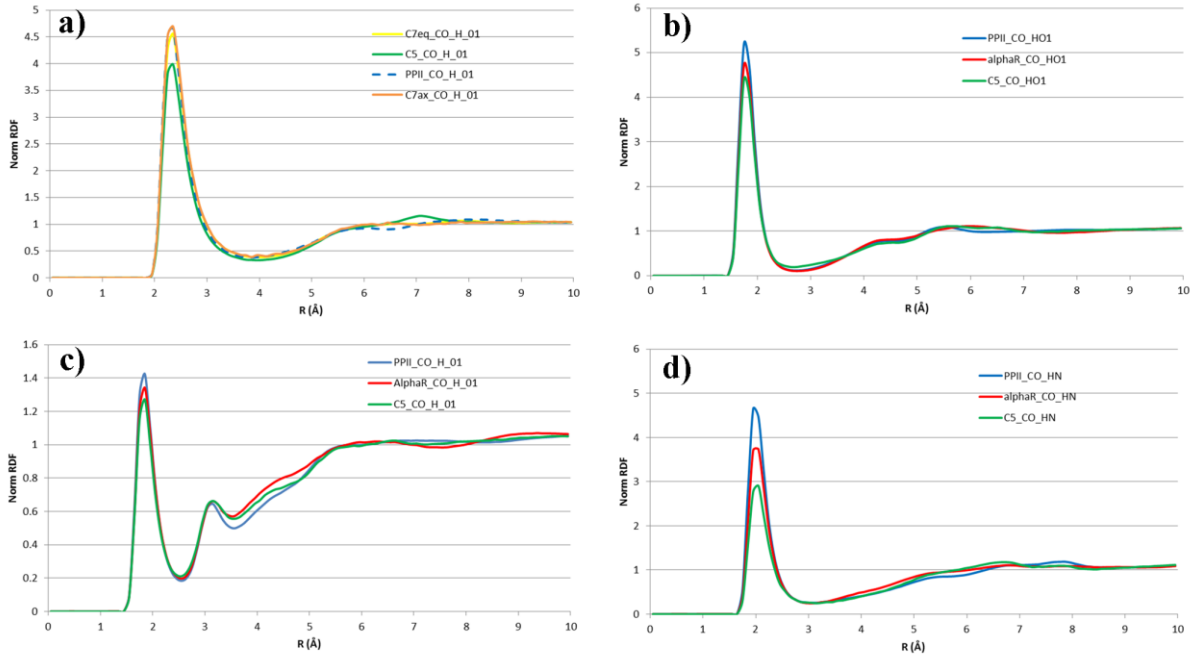

Figure 6.- Radial pair distribution function for the interaction between the acetyl carbonyl oxygen and a proton donor center of the solvent molecule for the PII, αR and C5 conformations. a) chloroform; b) methanol; c) water; d) NMA.

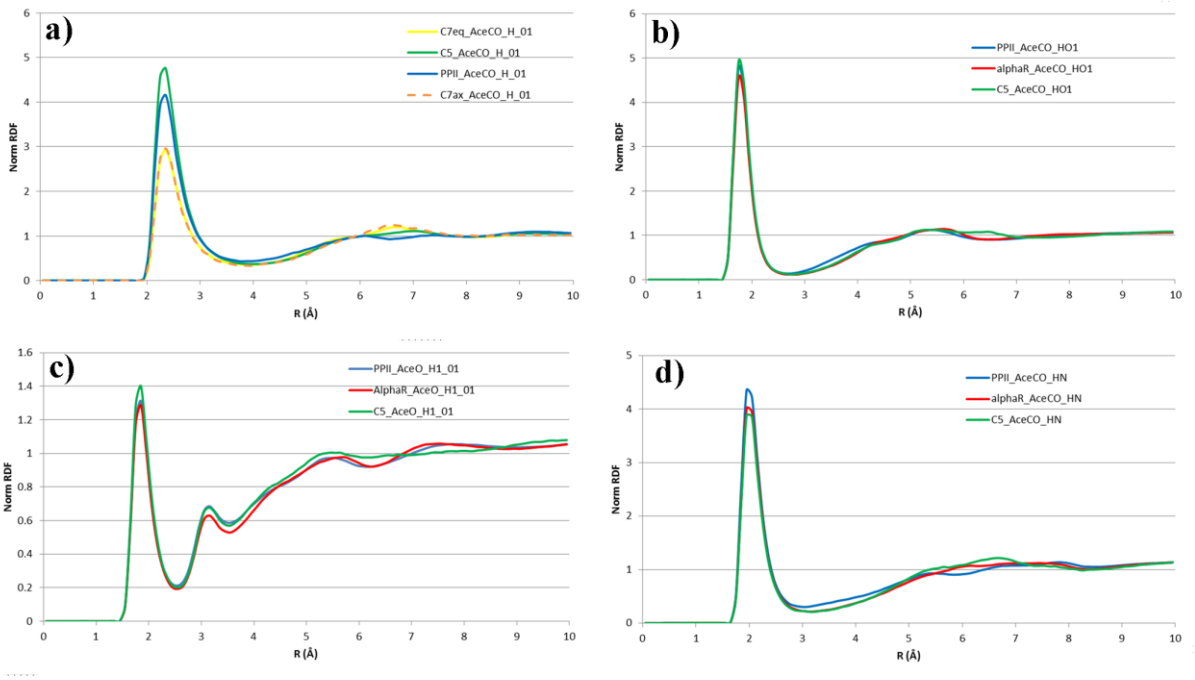

Figure 7.- Radial pair distribution function for the interaction between the alanine amide hydrogen and a proton accepting center of the solvent molecule for the PII, αR and C5 conformations. a) chloroform; b) methanol; c) DMSO; d) water; e) NMA.

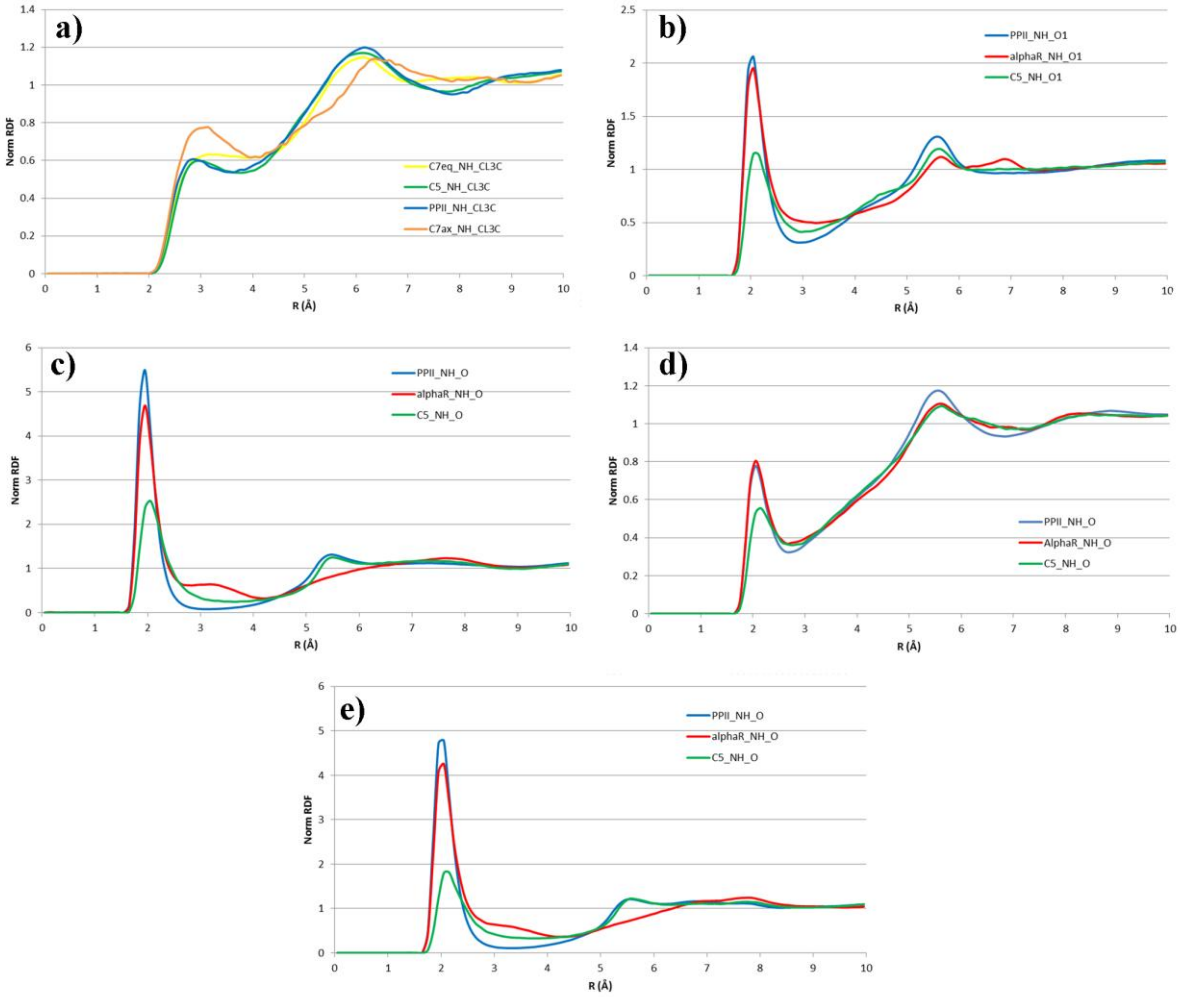

Figure 8.- Radial pair distribution function for the interaction between the N-methylamide hydrogen and a proton accepting center of the solvent molecule for the PII, αR and C5 conformations. a) chloroform; b) methanol; c) DMSO; d) water; e) NMA.

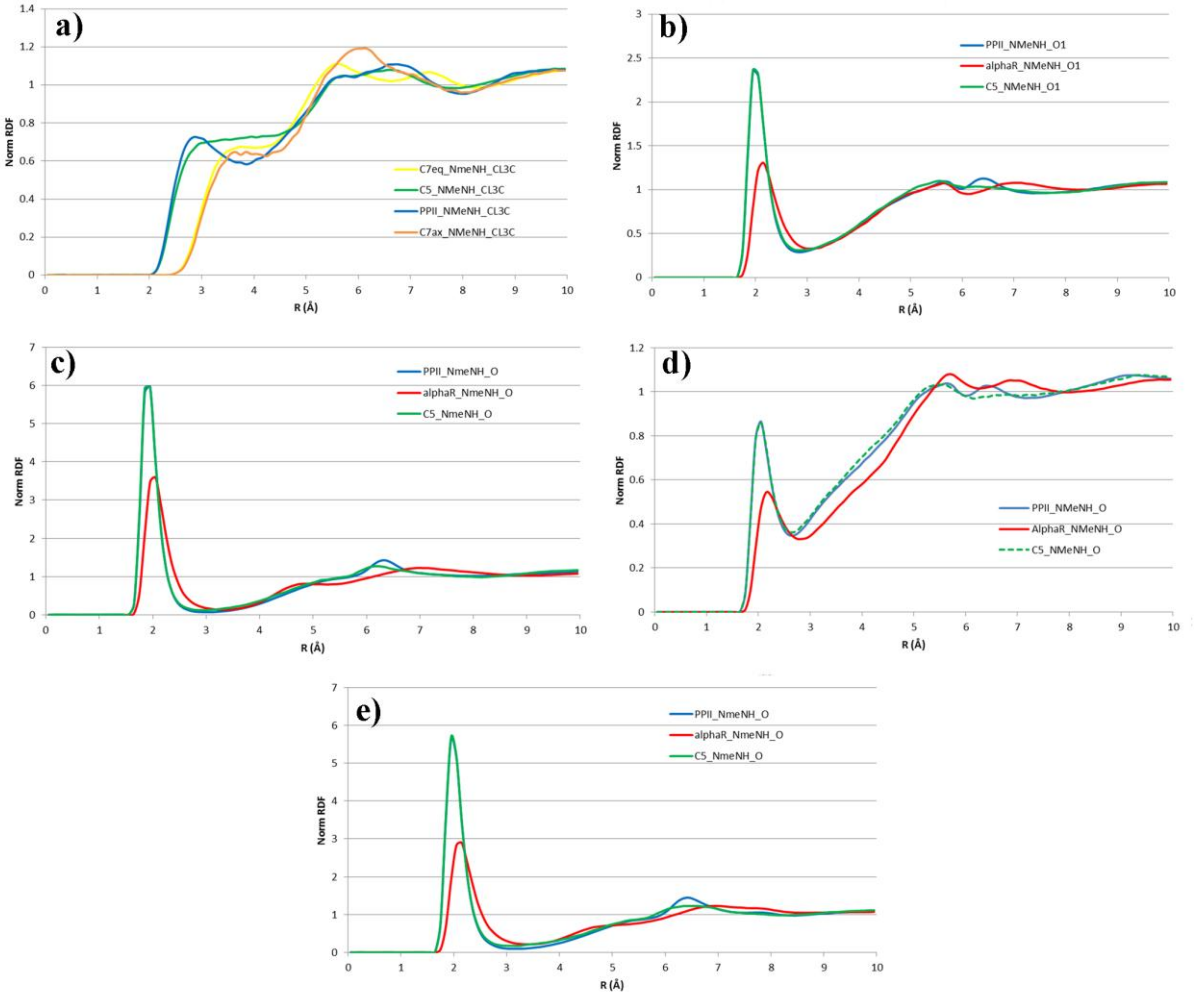

Table 1.- Conformational analysis of the alanine dipeptide deduced form MD calculations in explicit solvent. In the energy column numbers in parenthesis are the Boltzmann-weighted populations in percentage.

	CHCl3 explicit			**Methanol explicit**			**DMSO explicit**			**Water explicit**			**NMA explicit**		
	φ	ψ	Energy/ kcal mol^{-1}	φ	ψ	Energy/ kcal mol^{-1}	φ	ψ	Energy/ kcal mol^{-1}	φ	ψ	Energy/ kcal mol^{-1}	φ	ψ	Energy/ kcal mol^{-1}
C_7^{eq}	-80	50	0.00(46)												
C_5	-155	155	0.11(38)	-150	155	1.15(9)	-150	155	0.89(13)	-150	155	0.97(11)	-150	155	0.95(10)
PII	-75	140	0.89(10)	-75	150	0.00(61)	-70	150	0.00(58)	-70	150	0.00(59)	-70	150	0.00(49)
α_R				-75	-20	0.52(25)	-75	-20	0.52(24)	-75	-20	0.53(24)	-75	-20	0.18(36)
C_7^{axial}	60	-40	1.29(5)												
α'	-150	-50	4.82	-145	-5	1.74(3)	-145	-5	1.74(3)	-140	5	1.96(2)	-145	-15	1.35(5)
α_D	55	-145	4.86	60	165	4.01	60	165	4.01				55	170	4.65
β2															
α_L				55	20	2.07 (2)	55	20	2.07(2)	55	25	1.71(3)	55	20	2.48

Table 2.- Conformational analysis of the alanine dipeptide deduced form MD calculations using a generalized Born method. In the energy column numbers in parenthesis are the Boltzmann-weighted populations in percentage.

	CHCl3 implicit			Methanol implicit			DMSO implicit			Water implicit			NMA implicit		
	φ	ψ	Energy/ kcal mol^{-1}	φ	ψ	Energy/ kcal mol^{-1}	φ	ψ	Energy/ kcal mol^{-1}	φ	ψ	Energy/ kcal mol^{-1}	φ	ψ	Energy/ kcal mol^{-1}
C_7^{eq}				-80	80	2.47	-80	80	2.47						
C_5	-150	155	0.14(34)	-150	155	0.54(21)	-150	155	0.56(21)	-150	155	0.58(20)	-150	155	0.60(20)
PII	-75	150	0.00(43)	-70	150	0.00(52)	-75	150	0.00(52)	-70	150	0.00(53)	-75	150	0.00(53)
α_R	-75	-15	0.41(22)	-75	-20	0.40(27)	-75	-20	0.41(26)	-75	-20	0.41(27)	-75	-20	0.41(27)
C_7^{axial}				50	-100	5.19	60	-80	4.91	50	-115	4.79	50	-115	4.79
α'	-150	-90	5.00	175	-25	5.71	175	-35	5.72	-140	-105	5.34	-140	-105	5.34
α_D	55	-170	3.58	55	-175	3.45	60	-170	3.32	60	175	3.23	60	175	3.23
β2	-135	10	2.02	-135	5	1.94				-135	5	1.92	-135	5	1.92
α_L	55	20	2.02	55	25	2.22	55	25	2.07	55	25	2.03	55	25	2.03

.

Table 3.- Conformational analysis of the alanine dipeptide deduced form MD calculations using a bulk dielectric constant. In the energy column numbers in parenthesis are the Boltzmann-weighted populations in percentage.

	Vacuo ε=1.0			CHCl3 ε=4.8			Methanol ε=32.6			**DMSO ε=46.7**			**Water ε=78.5**			**NMA ε=191.3**		
	φ	ψ	Energy/ kcal mol^{-1}	φ	ψ	Energy/ kcal mol^{-1}	φ	ψ	Energy/ kcal mol^{-1}	φ	ψ	Energy/ kcal mol^{-1}	φ	ψ	Energy/ kcal mol^{-1}	φ	ψ	Energy/ kcal mol^{-1}
C_7^{eq}	-80	55	0.00 (69)															
C_5	-155	155	0.55 (28)	-155	150	0.00 (50)	-155	150	0.12 (38)	-155	150	0.13 (37)	-155	150	0.15 (36)	-155	150	0.17 (35)
PII				-75	145	0.16 (38)	-75	150	0.00 (46)	-75	150	0.00 (46)	-75	150	0.00 (47)	-75	150	0.00 (47)
α_R				-75	-15	1.05 (9)	-75	-20	0.93 (10)	-75	-20	0.93 (10)	-75	-20	0.94 (10)	-75	-20	0.93 (10)
C_7^{axial}	60	-45	1.89 (3)	60	-85	4.62	50	-120	4.70	50	-100	5.05	55	-110	4.83	50	-120	4.73
α'				-150	-5	1.87 (2)	-155	-10	1.15 (7)	-155	-10	1.12 (7)	-155	-10	1.08 (8)	-155	-10	1.06 (8)
α_D				60	165	3.41	60	160	2.46	60	160	2.38	50	-125	4.49	60	165	2.37
β2							175	35	5.29	175	25	4.87	175	50	5.64	175	50	5.18
α_L				55	15	2.28	55	25	1.99	55	25	1.96	55	25	1.92	55	25	2.00